Low-temperature electron-paramagnetic-resonance study of extrinsic and intrinsic defects in CuGaSe$_2$

M. Birkholz and P. Kanschat
Hahn-Meitner-Institut, Abteilung Photovoltaik, Rudower Chaussee 5, D-12489 Berlin, Germany

T. Weiss
Hahn-Meitner-Institut, Abteilung Photovoltaik, Abteilung Heterogene Materialsysteme, Rudower Chaussee 5, D-12489 Berlin, Germany

M. Czerwensky
Hahn-Meitner-Institut, Abteilung Photovoltaik, Bundesanstalt für Materialforschung und -prütung, Labor I. 13, Rudower Chaussee 5, D-12489 Berlin, Germany

K. Lips
Hahn-Meitner-Institut, Abteilung Photovoltaik, Rudower Chaussee 5, D-12489 Berlin, Germany
(Received 21 December 1998)

The low-temperature electron-paramagnetic resonance (EPR) of the compound semiconductor CuGaSe$_2$ was investigated. Spectra of as-grown lumps and powders with a defined maximum grain size were measured in X band. The spectra of two transition-metal impurities, Ni$^+$ and Fe^{2+}, could be identified and their appropriate EPR parameters are presented. The position of the Fermi-level energy within the forbidden zone as indicated by the occurrence of nickel and iron with these oxidation states is discussed by analogy with previous EPR investigations on other chalcopyrite semiconductors. An aging effect was observed, associated with the occurrence of EPR signals typical for Cu^{2+}. The nature of the aging process is discussed with respect to the electronic properties of CuGaSe$_2$ for thin-film solar cell applications. [S0163-1829(99)01019-X]

CuGaSe$_2$ is a representative of the class of *I-III-VI*$_2$ semiconducting chalcopyrites. The chalcopyrite structure is a tetragonal derivative from the cubic sphalerite structure. Two different bond lengths occur in the crystal lattice between metal and chalcogen atoms giving rise to a variety of interesting physical properties.[1] CuGaSe$_2$ exhibits its first fundamental transition via a direct band gap of 1.68 eV at RT. The optical absorption coefficient is larger than 10^4 cm^{-1} for $h\nu > 1.7$ eV. Electrical conduction in both crystals and thin films of CuGaSe$_2$, was always found p-type and experiments for n-type doping failed, although the material is generally recognized as electronically compensated. Charge carrier densities could be adjusted by adequate doping from 10^{12}–10^{19} cm^{-3}, while effective mobilities in single crystals were determined to range to about 80 cm^2 V^{-1} s^{-1} at room temperature.[2] These optical and electronic properties qualify CuGaSe$_2$ for absorber layer applications in thin-film solar cells and energy conversion efficiencies of 9.7% and 9.3% have already been achieved for single-crystal[3] and thin-film cells,[4] respectively.

The knowledge of intrinsic defects like stoichiometry deviations and extrinsic defects like unintentional doping are important prerequisites to understand the electronic properties of such a material and to identify strategies for device optimization. Electron paramagnetic resonance (EPR) is a powerful tool for this purpose and some dozen EPR investigations of chalcopyrite semiconductors have already been performed. These investigations mainly concentrated upon sulfur-containing wide-band-gap materials and lead to the identification of paramagnetic transition-metal impurities and stoichiometry deviations.[5–11] Later, selenium-based compounds were studied[12–16] that are also under investigation for solar cell applications. In this work we present EPR investi-

gations that were carried out on CuGaSe$_2$. In the course of the work we realized the occurrence of a large variety of EPR signals in CuGaSe$_2$, from which results are presented here.

Intentionally undoped CuGaSe$_2$ was synthesized from the elements as described previously.[17] Preparation, storing, and handling of the starting and synthesized material was either carried out in the inert gas atmosphere of a glovebox or under high-vacuum conditions. Stoichiometric mixtures of the elements (6N Cu, 7N Ga, 5N Se) were filled into vitreous carbon boats that were inserted in a quartz glass ampoule and evacuated. The ampoule was exposed to a two-step heating process at temperatures of 1100 °C for 6 h and 900 °C for seven days. Bulky, silver-shining, and brittle lumps were obtained by this procedure. X-ray-powder diffractograms of crushed and mortared material showed that single-phase CuGaSe$_2$ had been synthesized. Inductively coupled plasma mass spectroscopy (ICPMS) measurement revealed contamination by Li, Fe, Zn, Ag in the ppm range and by Ni in the sub-ppm range.[18] As-grown bulk material was polycrystalline and consisted of small and irregular oriented crystallites of sub-mm dimensions as was proven by von-Laue backscattering diffractometry. For EPR investigations samples were filled into Suprasil quartz glass tubes that were succeedingly evacuated to avoid oxygen contamination which is known to have a deteriorate effect on the electronic properties.[4] In order to obtain orientationally averaged spectra, some measurements were performed on powdered samples that had been mortared and passed through an 80-μm testing sieve. Experiments were performed in a Bruker Elexys 500 spectrometer operating at X band microwave frequencies. Samples were cooled in a helium flow cryostat to temperatures ranging from 5 K to RT. For orien-
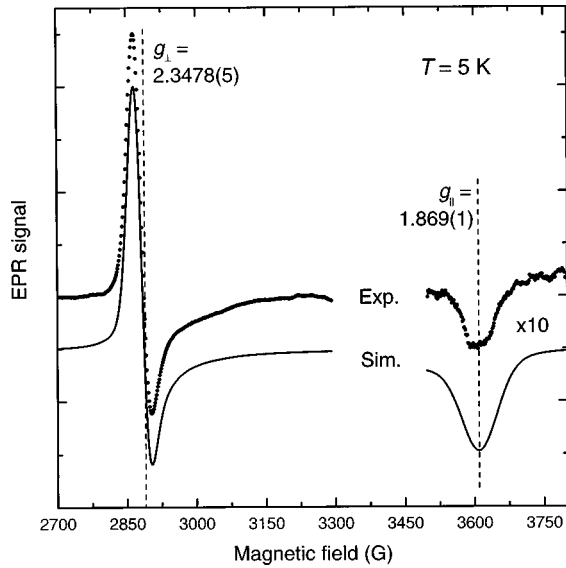
FIG. 1. Measured and simulated EPR spectra of CuGaSe$_2$ powder. The simulation was done by inserting the g values given in the plot and fixing the parallel and perpendicular linewidths to 38 and 76 G. The measured $S = \frac{1}{2}$ paramagnetic center is assigned to Ni$^+$.

FIG. 2. Orientation dependence of low-field signals measured in CuGaSe$_2$ lumps at 10 K [■ and ●, experiment; —, $1/\cos(\phi - \phi_0)$ fit]. The signals are assigned to paramagnetic Fe^{2+} centers. The insets display measured spectra for two selected orientations.

tation dependent measurements the spectrometer was equipped with a goniometer sample holder exhibiting its axis of rotation perpendicular to the static magnetic field.

Figure 1 displays a background-corrected powder spectrum of CuGaSe$_2$ measured at 5 K. A so-far unidentified some-hundred G wide Lorentzian signal at $g = 2.034$ and a narrow line with $\Delta H_{pp} < 1$ G at $g = 2.003$ were subtracted. The nature of both signals is currently under investigation and will not be considered here. We observed two structures at $g = 2.3478(5)$ and $1.869(1)$ that are typical powder spectra features for a $S = \frac{1}{2}$ system exhibiting an uniaxial g tensor having $g_\perp > g_\parallel$. The anisotropic spectrum could well be simulated by fixing the line positions to the values given above and the perpendicular and parallel component of the linewidth to $\Delta H_{pp} = 38$ and 76 G, respectively, assuming a Gaussian line shape. Due to an increase of linewidth with increasing temperature, the signal could not be observed for $T > 40$ K.

The signal is assigned to Ni$^+$ ions ($3d^9$) residing on one of the metal lattice sites, most probably on a copper site. On a metal lattice site the Ni$^+$ free ion's ground state ^2D is split by the cubic and tetragonal components of the crystal field, accounted for by the energy parameters $10Dq$, δ, and μ, and by spin-orbit coupling into five Kramer doublets. Preceding EPR work on the related sulfur compound CuGaSe$_2$ that was intentionally doped with nickel revealed the lowest energy state of Ni$^+$ to be the $^2B^a$ level.[9] The structural parameters in the selenide differ by less than 5% from those encountered by the sulfide[19,20] and we therefore assume the nickel's lowest-energy state to be the same in both host lattices. Our assignment of the axial-symmetric center to Ni$^+$ in the selenide is confirmed by the close agreement of g values, linewidths, and their temperature dependence compared to the values encountered in the sulfide.[9,21,22] Finally, the density of paramagnetic centers amounted to about 0.5 ppm which was found to correspond with the nickel concentration as determined by inductively coupled plasma mass spectroscopy (ICPMS).
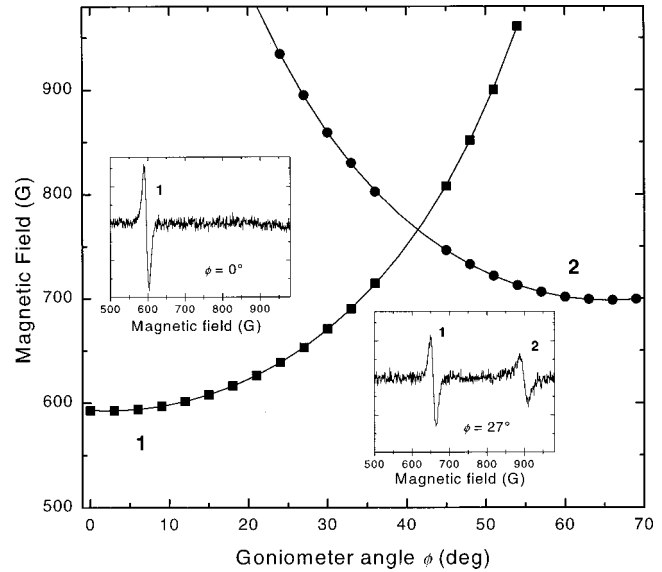
It is of interest to compare measured g values of the Ni$^+$ center in CuGaSe$_2$ with those in CuGaS$_2$, the latter of which were reported as $g_\perp = 2.3243(10)$ and $g_\parallel = 1.9185(15)$.[22] The deviation of g-tensor components from the free electron value of $g_e = 2.0023$ is seen to increase on descending from the sulfide to the selenide. This effect may qualitatively be understood in terms of the ionic model. Although the model takes an oversimplified view it generally predicts the right tendencies. Within this model the cubic splitting factor $10Dq$ is proportional to $1/R^5$, with R accounting for the distance from Ni to the four nearest chalcogen neighbors. Considering the formulas as derived by Kaufmann,[9] $(10Dq)^{-1}$ is realized to be the principal component adjusting the deviation of $g_\perp$ and $g_\parallel$ from g_e, while the tetragonal splitting factors μ and δ are only of minor importance. Since the nickel-chalcogen distance R is larger in the selenide than in the sulfide, $(10Dq)^{-1}$ should increase as should the deviation of both g components from the free-electron value. This is in accordance with our experimental results.

A second prominent signal could only be observed in as-grown polycrystalline CuGaSe$_2$ lumps. The signal showed a characteristic dependence upon orientation with respect to the static magnetic field that varied like $1/\cos \phi$, where ϕ accounts for the angle between H_0 and a symmetry axis in the material. The minimum resonance field Min(H_{res}) or maximum g_{eff} were found in the range of about 600 G or 10, respectively. Figure 2 displays the orientation dependence of two such signals originating from two different large crystallites contained in the lump, while the insets show the raw spectra that were measured at 10 K. Since crystalline lumps were rather unshapely, we were not in the position to identify the orientation of certain crystallographic faces or directions from their appearance. In order to elucidate the nature of the observed EPR line the crystal orientation was systematically changed to identify the minimum resonance field. We found Min(H_{res}) = 592 G which is equivalent to $g_{eff} = 11.34$ for a 9.45 GHz microwave frequency. The linewidth ΔH_{pp} exhibited a strong dependence upon orientation attaining its mini-

mum value of 16 G at $\text{Min}(H_{\text{res}})$.

We assign the signal to Fe^{2+} impurities residing on metal lattice sites. For an analysis we used the theoretical EPR formalism as developed[23] for tetrahedral Co^{3+}. The Fe^{2+} center in a chalcopyrite compound was first observed by Kaufmann in $CuAlS_2$,[24] followed by its identification in $CuInSe_2$ (Refs. 13 and 25) and $CuInS_2$.[16] The Fe^{2+} high spin configuration is that of a half filled $3d$ shell with a surplus electron. The free ion ground state ^5D is split by the cubic and tetragonal components of the crystal potential comparable to the situation encountered by Ni^+ and described by the splitting parameters $10Dq$, δ, and μ. Since Fe^{2+} is an even-electron system, important differences arise, however. For positive μ the lowest energy state is $^5B^a$ with $S=2$ which is split by spin-orbit coupling into $M_S=0$, ± 1, and ± 2 states separated by D and $3D$, respectively. The doublet $M_S=\pm 2$ is the lowest in energy and is finally split into $|2\rangle$ and $|\bar{2}\rangle$ states, the separation of which is proportional to the fourth-order cubic term a of the crystalline potential.

Since the energy associated with a is of the same order of magnitude as the energy of the magnetic splitting and the microwave quanta used in the EPR experiment, $|2\rangle$ and $|\bar{2}\rangle$ states cannot be considered as undisturbed. In the presence of the static magnetic field H_0 the eigenfunctions are formed by linear combinations of $|2\rangle$ and $|\bar{2}\rangle$. It is between these new levels that the microwave absorption is observed in the experiment. It can be shown by a calculation of transition matrix elements that only the $g_{\parallel}$ component may be observed while the $g_{\perp}$ component is shifted to infinitely large H_{res} fields and the signal shows its characteristic $1/\cos\phi$ orientation dependence.[23] Under the assumption that D is much larger than a and the absorbed microwave quanta $h\nu$, the resonance condition reads $(h\nu)^2=(4g_{\parallel}\mu_B H_{\text{res}})^2+a^2$, where $H_{\text{res}}=H_{\parallel}/(\cos\theta\cos\phi)$. Only the angle ϕ is varied in a goniometer experiment, while the inclination angle θ of the c axis towards H_0 has to be identified by successively changing it. We determined the two free parameters in the resonance equation by systematically changing the microwave frequency and the orientation of the lump with respect to H_0 and found $a=0.208(1)$ cm^{-1} and $g_{\parallel}=2.14(3)$. These values are in the typical range of previously reported values for Fe^{2+} in other chalcopyrite compounds.[13,16,24,25] The observation of iron impurities in our as-grown material can be understood from the spurious contamination of the starting material, i.e., $6N$ copper and $5N$ selenium.

In previous EPR investigations on $CuInSe_2$ (Refs. 13 and 25) and $CuInS_2$ (Ref. 16) Fe^{2+} could be identified in vacuum-annealed material, while in as-grown material iron contaminations were observed[5,6,8,12,26–28] as three-valent Fe^{3+}. The effect may qualitatively be understood from a shift of the Fermi-level energy E_F by the annealing procedure causing a selective loss of the high vapor-pressure component of the compound, being sulfur or selenium in the cases considered here. In a simplified picture, group VI vacancies in II-VI and I-III-VI_2 semiconductors may be assumed to act as donors. Their enrichment in vacuum-annealed samples would consecutively lead to a shift of E_F towards the conduction-band edge favoring n-type conduction. Although these arguments are only of qualitative na-
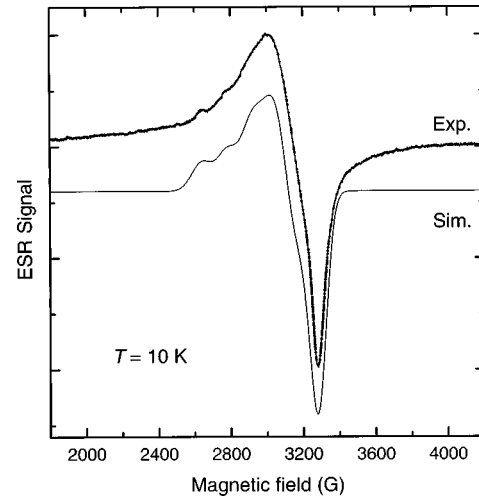
FIG. 3. EPR difference spectra of $CuGaSe_2$ powder that was obtained by subtracting the spectrum of a freshly mortared sample from a spectrum of the same sample after six weeks of aging. The large hyperfine-broadened signal is assigned to the Cu^{2+} paramagnetic center, which is simulated with EPR parameters given in the text.

ture, they gained experimental support from the investigations on chalcopyrite semiconductors. Nickel and iron contaminants in other semiconducting chalcopyrites were found to occur with varying valencies.[7–9,13,16,27] In the case of nickel both paramagnetic ions Ni^+ and Ni^{3+} and in the case of iron Fe^{2+} and Fe^{3+} have been identified and especially in $CuGaS_2$ their relative concentration was realized to monitor stoichiometry deviations.[8] Even the position of the Fermi level could qualitatively be followed by the observation of differently prepared samples.[27] In the course of these investigations, the position of the Fe^{2+}/Fe^{3+} demarcation level in $CuInSe_2$ was identified close to the middle of the gap.[25] Having these results in mind, the observation of Fe^{2+} by EPR in $CuGaSe_2$ is consistent with previous investigations, but appears surprising at the same time. On the one hand, the observation of Fe^{2+} is consistent with earlier investigations, since lump material was grown under quasi-vacuum-annealing conditions. On the other hand, the observation of both nickel and iron in such low oxidation states Ni^+ and Fe^{2+} instead of Ni^{3+}/Fe^{3+} in $CuGaSe_2$ appears surprising, since it may concluded by analogy with previous investigations that the Fermi-level energy is not situated close to the valence band edge but lies distinctively above it. This was not to be expected for usually low-resistivity p-type material.

The third paramagnetic center identified in $CuGaSe_2$ merely occurred after exposure to air and appeared as an aging effect. As was pointed out above, material processing and preparation was almost completely done in an inert gas atmosphere or in vacuum. A difference spectrum is depicted in Fig. 3 that was obtained by subtracting two spectra of the same sample recorded two days and six weeks after preparation of the powder. The sample was shortly exposed to air while filling it into the EPR quartz tube, but it was stored in an inert gas atmosphere before and in the high-vacuum evacuated and sealed tube afterwards. We assume the difference spectrum to contain only the signal caused by the aging effect.

The signal is broadened by an unresolved hyperfine inter-

action splitting and it compares very well with the typical signature of Cu^{2+} ($S = \frac{1}{2}$) EPR powder spectra, see for instance Refs. 29–31. Copper naturally occurs as ^{63}Cu and ^{65}Cu both having $I = \frac{3}{2}$ and causing the EPR spectra of single crystals to contain groups of four lines. The measured g tensor of Cu^{2+} is generally rhombic, i.e., three distinctive components in its diagonal form, which holds for many coordination geometries among them the planar and tetrahedral ones and the distorted derivatives from both. We simulated the measured difference spectrum and determined the EPR parameters of Cu^{2+} in air-exposed $CuGaSe_2$ to be $g_{xx} = 2.07(1)$, $g_{yy} = 2.18(2)$, $g_{zz} = 2.40(5)$, and the hyperfine coupling constants $A_{xx} = A_{yy} \approx 30$ and $A_{zz} = 140(5)$ G. The simulated spectrum is shown in the lower part of Fig. 3. Although the parameters' precision is low due to strong broadening by spherical averaging, large linewidths, etc., they lie clearly in the typical range of EPR parameters g and A of Cu^{2+}.[29–31] The assignment of Cu^{2+} as source of the difference signal is corroborated by the high spin density of the center which could only be caused by the conversion of one of the previously EPR-quiet ions intrinsically contained in the sample, i.e., Cu^+, Ga^{3+}, or Se^{2-}.

It has to be emphasized that a simulation of the measured spectra by means of an axial symmetric g tensor was not possible. A distinction between xx and yy components had to be introduced in order to arrive at reliable simulations of the measured data. The tensor symmetry therefore indicates that Cu^{2+} ions have a coordination symmetry different from copper ions in native $CuGaSe_2$ which bonding symmetry is S_4 and which formal valency is $+1$. We therefore conclude that for a number of copper ions in aged $CuGaSe_2$ both the formal valency and the bonding symmetry deviate from their usual values in the material unexposed to air. We propose to understand the effect in terms of a redox reaction involving surface copper ions. Airborne oxygen may be imagined to cause an oxidation of the copper ions at the crystal surface. If oxygen is assumed to be bonded to surface copper ions the variation of both properties of copper as signaled by EPR spectra may be understood. The valency change would be caused by the second ionization of copper, while the symmetry distortion would be due to the coordination of copper to oxygen in the neighborhood. In this context it is of interest to realize that a pronounced degradation n-CdS/p-$CuGaSe_2$ solar cells was observed when $CuGaSe_2$ absorber layers were exposed to air prior to deposition of the buffer layer.[4] We speculate that the microscopic mechanism of this degradation process may be understood in terms of a copper oxidation as it was observed in our measurements.

In conclusion, we have presented the first low-temperature EPR measurements of as-grown and aged $CuGaSe_2$. We identified three paramagnetic centers Ni^+, Fe^{2+}, and Cu^{2+} and gave their respective g- and A-tensor components. Determined g values of Ni^+ and Fe^{2+} could be understood by comparison with values as measured in other chalcopyrite compounds. The occurrence of Ni^+ and Fe^{2+} signals may indicate the Fermi level to lie distinctively above the valence band edge in our material. This result appears surprising for $CuGaSe_2$ that has solely been found to be p-type so far. Air-exposed material was found to develop an aging signal that could be identified to be due to Cu^{2+}. The effect is proposed to be understood in terms of an oxidation of copper ions close to the crystal surface which may be of importance for solar cell and other intended optoelectronic applications of $CuGaSe_2$.

[1] J. L. Shay and J. H. Wernick, *Ternary Chalcopyrite Semiconductors: Growth, Electronic Properties, and Applications* (Pergamon Press, Oxford, 1975).

[2] J. H. Schön, F. P. Baumgartner, E. Arushanov, H. Riazi-Nejad, C. Kloc, and E. Bucher, J. Appl. Phys. **79**, 6961 (1996).

[3] M. Saad, H. Riazi-Nejad, E. Bucher, and M. C. Lux-Steiner, in *1st World Conference on Photovoltaic Energy Conversion* (IEEE, Hawaii, 1994), p. 214.

[4] V. Nadenau, D. Hariskos, and H. W. Schock, in *14th EC Photovoltaic Solar Energy Conference*, edited by H. Ossenbrink, P. Helm, and H. Ehmann (Stephens & Associates, Barcelona, 1997), p. 1250.

[5] J. Schneider, A. Räuber, and G. Brandt, J. Phys. Chem. Solids **34**, 443 (1973).

[6] G. Brandt, A. Räuber, and J. Schneider, Solid State Commun. **12**, 481 (1973).

[7] U. Kaufmann, A. Räuber, and J. Schneider, Solid State Commun. **15**, 1881 (1974).

[8] H. J. von Bardeleben, A. Goltzene, and C. Schwab, J. Phys. Colloq. **36**, C3 (1975).

[9] U. Kaufmann, Phys. Rev. B **11**, 2478 (1975).

[10] H. J. von Bardeleben, A. Goltzene, and C. Schwab, Phys. Status Solidi B **76**, 363 (1976).

[11] G. L. Troeger, R. N. Rogers, and H. M. Kasper, J. Phys. C **9**, L73 (1976).

[12] H. J. von Bardeleben and R. D. Tomlinson, J. Phys. C **13**, L1097 (1980).

[13] J. M. Tchapkui-Niat, A. Goltzene, and C. Schwab, J. Phys. C **15**, 4671 (1982).

[14] G. K. Padam, G. L. Malhotra, and S. K. Gupta, Sol. Energy Mater. **22**, 303 (1991).

[15] Y. J. Hsu and H. L. Hwang, J. Appl. Phys. **66**, 5798 (1989).

[16] N. Nishikawa, I. Aksenov, T. Shinzato, T. Sakamoto, and K. Sato, Jpn. J. Appl. Phys., Part 2 **34**, L975 (1995).

[17] T. Weiss, M. Birkholz, Y. Tomm, A. Jäger-Waldau, and M. C. Lux-Steiner, J. Cryst. Growth (to be published).

[18] R. Matschat and M. Czervensky (unpublished).

[19] S. C. Abrahams and J. L. Bernstein, J. Chem. Phys. **59**, 5415 (1973).

[20] S. C. Abrahams and J. L. Bernstein, J. Chem. Phys. **61**, 1140 (1974).

[21] H. J. von Bardeleben, C. Schwab, and A. Goltzene, Phys. Lett. **51A**, 460 (1975).

[22] G. L. Troeger, R. N. Rogers, and H. M. Kasper, J. Phys. C **8**, L222 (1975).

[23] M. D. Sturge, F. R. Merritt, J. C. Hensel, and J. P. Remeika, Phys. Rev. **180**, 402 (1969).

[24] U. Kaufmann, Solid State Commun. **19**, 213 (1976).

[25] K. Sato, N. Nishikawa, I. Aksenov, T. Shinzato, and H. Nakanishi, Jpn. J. Appl. Phys., Part 1 **35**, 2061 (1996).

[26] H. J. von Bardeleben, A. Goltzene, C. Schwab, and R. S. Feigelson, Appl. Phys. Lett. **32**, 741 (1978).

[27] I. Aksenov and K. Sato, Jpn. J. Appl. Phys., Part 1 **31**, 2352 (1992).

[28] I. Aksenov, N. Nishikawa, and K. Sato, J. Appl. Phys. **74**, 3811 (1993).

[29] I. H. Parker, J. Phys. C **4**, 2967 (1971).

[30] F. J. Owens, J. Appl. Phys. **53**, 368 (1982).

[31] S. K. Hoffmann, J. Goslar, and L. S. Szczepaniak, Phys. Rev. B **37**, 7331 (1988).